PRACTICAL RESULTS AND PROSPECTS OF USING FIBER OPTICAL SENSORS OF ACOUSTIC EMISSION FOR DIAGNOSTING THE TECHNICAL CONDITION OF AIRCRAFT UNITS

DOI: 10.36724/2072-8735-2021-15-12-52-61

Dmitry S. Koptev,
Southwest State University, Kursk, Russia,
d.s.koptev@mail.ru

Ivan E. Mukhin,
Southwest State University, Kursk, Russia,
makskatol21@yandex.ru

Manuscript received 17 November 2021;
Accepted 15 December 2021

Keywords: *acoustic emission, fiber-optic acoustic emission sensor (FOAES), Doppler effect, fiber-optic Bragg gratings (FOBG), inclined Bragg grating (IBG), partially inclined Bragg cell (PIBC)*

Peripheral sensors for measuring aircraft parameters are an integral part of any system for diagnostics and forecasting of technical condition. Their principle of operation in relation to operation at aviation complexes is to convert mechanical, electromagnetic or light quantities into electrical ones for their subsequent processing. The process of radiation of disturbances propagating in the material caused by the dynamic local rearrangement of the structure of materials under the action of internal stresses leading to a change in the crystal lattice or the movement of micro- and / or macrodefects is called acoustic emission. So, the analysis of differences in the form of acoustic waves allows the classification of the type of deformation: crack or plastic deformation, which allows you to more accurately determine the current state of the airframe or diagnosed nodes. The principle of operation of such sensors is based on the effect of converting the linear dimensions of a Bragg cell, made on an optical fiber, into a change in the reflected wavelength. A necessary condition for obtaining correct results of measurements of stress states is the need for temperature compensation of the Bragg cells, which is achieved by introducing additional cells that are mechanically decoupled from the material being diagnosed and react only to the temperature component. The advantage of this method is the absence of the need for additional adjustment of the cells and their alignment, as well as the independence of measurements from the effects of electromagnetic radiation; the sensors are lightweight, vibration-resistant, and insensitive to electromagnetic fields. The article presents the practical results of using fiber-optic acoustic emission sensors for diagnosing the technical condition of critical components and assemblies of aircraft, as well as outlines the prospects for their deepest integration into a unified information and analytical system for diagnosing and predicting the technical state of aviation complexes. The developed technical solutions aimed at simplifying the methods of processing broadband acoustic emission signals, which make it possible to design acoustic emission sensors based on optical fiber, are structurally simpler and cheaper, with an increased signal-to-noise ratio, due to one conversion of an acoustic-optical signal into an electrical one.

Information about authors:

Dmitry S. Koptev, *Senior Lecturer, Department of Space Instrumentation and Communication Systems, Southwest State University, Kursk, Russia*

Ivan E. Mukhin, *Doctor of Technical Sciences, Senior Researcher, Professor of the Department of Space Instrumentation and Communication Systems, Southwest State University, Kursk, Russia*

Для цитирования:

Коптев Д.С., Мухин И.Е. Практические результаты и перспективы использования волоконно-оптических датчиков акустической эмиссии для диагностики технического состояния агрегатов летательных аппаратов // T-Comm: Телекоммуникации и транспорт. 2021. Том 15. №12. С. 52-61.

For citation:

Koptev D.S., Mukhin I.E. (2021) Practical results and prospects of using fiber optical sensors of acoustic emission for diagnosting the technical condition of aircraft units. *T-Comm*, vol. 15, no.12, pp. 52-61. (*in Russian*)

Introduction

In addition to strain gauges widely used in static tests, which have a relatively low reliability, currently intensive research is being carried out in the field of acoustic emission (AE) sensors based on optical fiber. For the successful implementation of the AE method in the control and diagnostics of products made of polymer composite materials (PCM), noise-immune devices and converters, software and methodological support and the creation of certain conditions for testing are required, due to the fact that AE in composite materials strongly depends on the radiation of the matrix. reinforcing filler, the relationship of the matrix and filler.

Materials and research methods

To select the type of AE sensor and build an optimal circuit of the measuring device, it is necessary to determine the minimum and maximum number of arising AE pulses, their energy and frequency range.

The level of interference signals affecting the AE sensor is significantly affected by the directivity characteristic of the AE sensor. From this, the following conclusions can be drawn [1]:

1) hen using the AE method for detecting and recording the moment of nucleation (starting) or studying the kinetics of the development of cracks (defects), directional AE sensors are effective;

2) hen using the AE method to study the destruction process in the entire volume of a structural material or product, non-directional AE sensors are most effective.

Taking into account the wide spectrum of AE signals (from 30 to 3000 kHz) and small amplitudes of sensor displacements from the AE signals (from 10^{-7} to 10^{-4} m), broadband and highly sensitive AE transducers are required. An important condition for the application of the AE method is the minimum level of the intrinsic noise of the transducer. The intrinsic noise of the AE piezoelectric transducers consists of breakdown noise, Barkhausen noise, mainly of cyclic polarization reversal noise. Also, an important condition is to minimize the influence of electrical and electromagnetic interference, so an increased noise immunity of the AE measuring transducers is required.

To minimize distortions of the AE signals, the natural resonance frequency of the AE sensor should be higher than the maximum transmission frequency of the receiving amplifying channel. The method of application of the AE method depends on the type of the AE transducer and the type of material or product being inspected.

It should be noted that the current regulatory documents are not aimed at controlling a specific type of product, which often hinders the use of the objectively unique capabilities of the AE control method.

A fiber-optic acoustic emission sensor (FOAES) is very suitable as an AE sensor, in particular based on the intra-fiber Doppler effect and fiber Bragg gratings (FOBG), the former belong to the category of non-directional AE sensors, and the latter are directional.

Diffraction fiber-optic sensors based on fiber Bragg gratings (FOBG) are based on the effect in which the wavelength of the reflected light peak is proportional to the measurement of the Bragg lattice pitch, which is determined by deformation and temperature. The amount of deformation of composite materials is determined by the magnitude of the shift of the wavelength of the signal peak.

The shift of the peak of the FOBG wavelength λ_w occurs linearly (within the range of Hooke's law for quartz glass) and is directly proportional to the deformation [2]:

$$\frac{\Delta\lambda_B}{\lambda_B} = (1-\rho_\alpha)\cdot\Delta\varepsilon', \quad (1)$$

where $\Delta\varepsilon$ – deformation, mk $\cdot 10^{-6}$;

ρ_α – the coefficient of photoelasticity (0.21 for SiO_2).

At λ_w = 1.31 μm and a temperature of 20 ° C, the FOBG sensitivity is 1 pm $\cdot 10^{-6}$.

The strict dependence of the shift of the peak wavelength λ_w on deformation and temperature has the following form:

$$\Delta\lambda_B = 2n\Lambda\left(\left\{1-\left(\frac{n^2}{2}\right)\left[P_{12}-v\left(P_{11}+P_{12}\right)\right]\right\}\varepsilon+\left[\alpha+\frac{\left(\frac{dn}{dT}\right)}{n}\right]\right), \quad (2)$$

where P_{ij} – Pockels coefficients of the photoelastic tensor;

v – number Pausson;

α – the coefficient of linear thermal expansion;

ΔT – temperature change;

n – the refractive index;

Λ – the step of the Bragg lattice.

Sensors based on FOBG are convenient in that their signal has a high signal-to-noise ratio, high sensitivity to deformations, they allow interrogating one fiber and multiplexing many fiber-optic sensors (up to 10 thousand pieces), and can have three-axis deformation sensitivity. For example, FOBG with multi-axis sensitivity is used to detect damage in composite pressure vessels.

Unlike FOBG, Doppler FOAES is non-directional. The use of several Doppler FOAESs, as shown in Figure 1, allows, by temporal processing, to combine the responses to the ultrasonic AE signal and form the radiation pattern of the Doppler FOAES system, as shown in Figure 2.

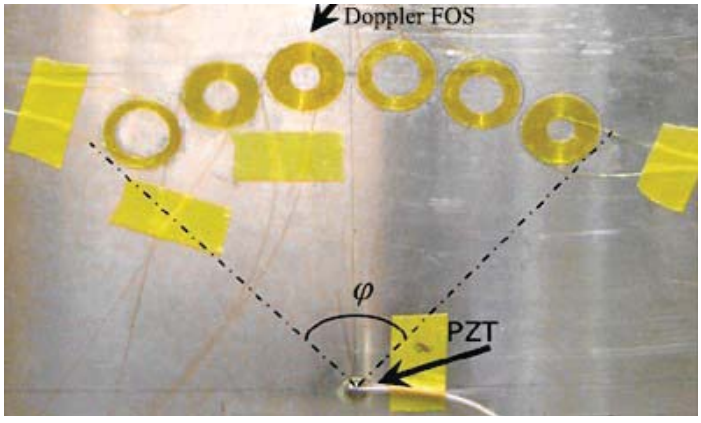

Figure 1. Array of Doppler FOAES on an aluminum plate

This figure shows a battery of optical fiber ring sensors. Each of them allows you to measure the acoustic wave caused by inhomogeneity or defect in the controlled sample (product). Using the results of several measurements will allow you to localize the location of the defect.

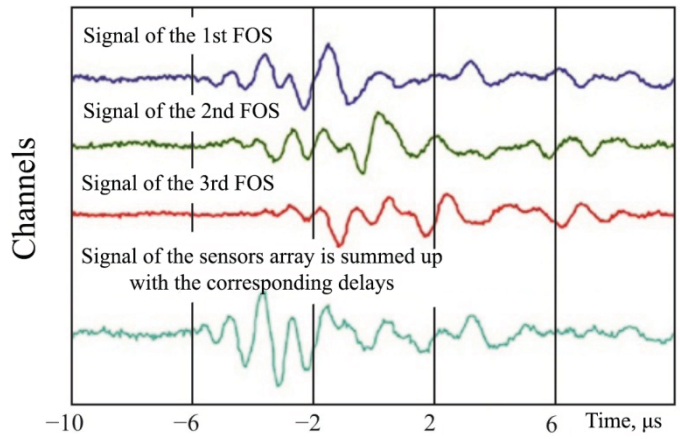

Figure 2. Combination (phasing) of FOAES signals during processing

In addition to accurately locating the defect, the use of signals from multiple fiber optic sensors can significantly increase the detection sensitivity of acoustic emission signals, as shown in the lower curve in Figure 2.

Monitoring of aircraft structures made of PCM is most effective using FOAES due to the natural properties of Doppler FOAES - compactness, noise immunity, broadband (without resonances from 10 kHz to 10 MHz) and high sensitivity with a dynamic range of up to 160 dB, a wide temperature range up to 500°C, high reproducibility parameters and their complete independence from the influence of temperature: temperature change does not affect the optical frequency of the intra-fiber signal.

The directional diagram of the FOAES based on the FOBG is determined by the ratio of the length of the Bragg grating and the length of the acoustic wave. If the FOBG length is much less than the acoustic wavelength, then the FOAES is practically omnidirectional, but if the FOBG length (in our case, from 5 to 25 mm) is greater than the acoustic wavelength, then directional properties appear. For FOBG, this is associated with the formation of an additional acoustic wave inside the quartz-fiber, which has a higher propagation velocity (about 3600 m/s) compared to the speed of the acoustic wave in the PCM. This leads to the addition of their effect at angles of about ± 30 degrees relative to the normal and the formation of a corresponding directional pattern (Fig. 3).

Using FOBG of different lengths and soundproof metallized coatings of the optical fiber, it is possible to create the required diagram of such FOAES.

As a result of the study of the materials considered, it follows that the most promising fiber-optic acoustic emission sensors (FOAES) are FOAES of the frequency type, based on the effect:

– modulation of the optical frequency of the reflection signal from the Bragg diffraction grating;

– modulation of the fiber laser radiation frequency;

– Intraluminal Doppler shift of the optical frequency under the action of acoustic waves.

Unlike a fiber Bragg grating, a Doppler fiber-optic acoustic emission sensor is non-directional. This property can be used to form the required radiation pattern when using several such sensors located at some distance from each other. Monitoring of aircraft structures with such sensors will make it possible to detect the beginning of the manifestation of irreversible deformations over a vast area that significantly exceeds the location of such sensors.

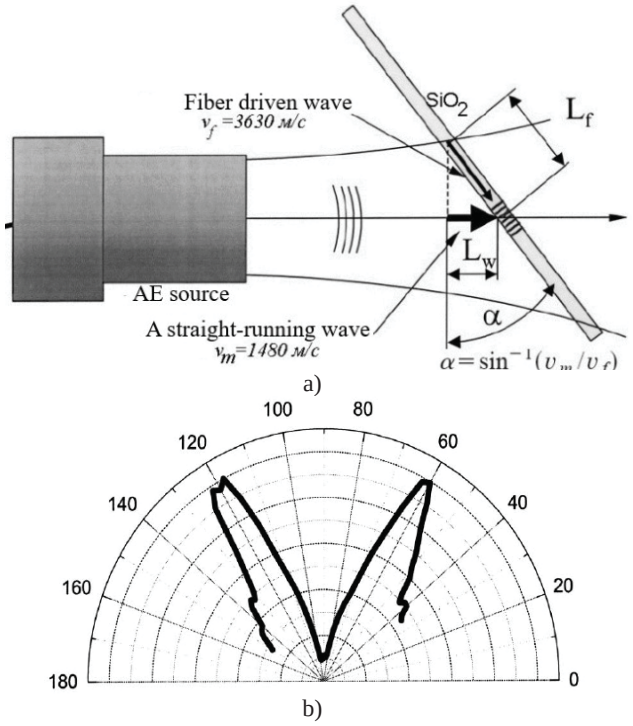

Figure 3. Directional diagrams of FOAES based on FOBG:
a – geometry of angular interaction of FOBG with an acoustic wave;
b – directional diagram of FOAES with angular geometry

The principle of operation of FOAES is based on the recently discovered intra-fiber Doppler effect [3], which consists in the fact that the frequency of the light wave f_0 radiation of a laser diode, passed through a bent optical fiber of length L, is shifted under the action of acoustic pressure. A fiber moves or vibrates at a speed dL/dt in an annular fiber Doppler element (Fig. 4) by the value f_d:

$$f_D = -\frac{n}{\lambda_0}\frac{dL}{dt}, \qquad (3)$$

where n – the refractive index of the optical fiber; λ_0 – the wavelength of light in the fiber.

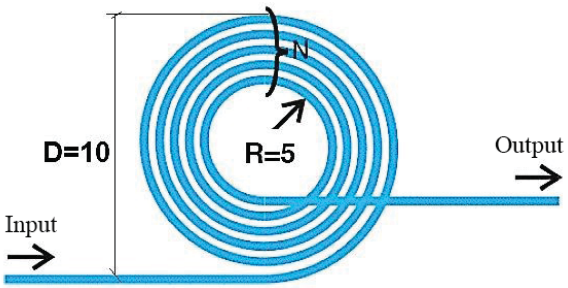

Figure 4. Configuration of the ring Doppler element

When the fiber is rolled into a ring and glued to the surface under study, the effect of detecting acoustic emission signals occurs. This effect is based on minor vibrations of the optical fiber ring from an acoustic wave, the appearance of the Doppler effect, and a change in the wavelength passing through the optical fiber ring of laser radiation, and this, in turn, is a sign of a defect in the material under study.

The Doppler shift of the optical frequency (Hz) in the annular element caused by deformations (movements) ε_x and ε_y is d efined as

$$f_D = -\frac{N\pi R_a n_э}{\lambda_0}(\varepsilon_x + \varepsilon_y) = -\frac{N\pi D_a n_э}{\lambda_0}(\varepsilon_x + \varepsilon_y), \quad (4)$$

where R_a – average radius of the fiber ring, mm; N – the number of fiber turns; n_e – equivalent refractive index.

Ring FOAES has no directional sensitivity. Nevertheless, if it is necessary to give it an appropriate directional pattern (for detecting and registering the moment of initiation or studying the kinetics of the development of cracks, defects), it can be U-shaped or elliptical, as shown in Figure 5.

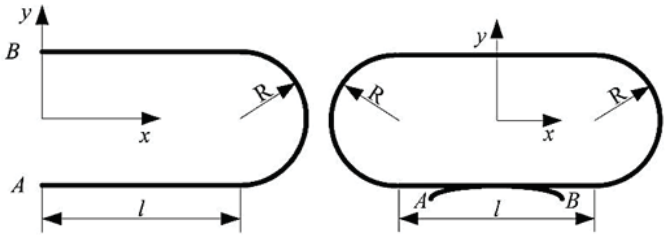

a) b)

Figure 5. Doppler fiber sensor configurations:
a – U-shaped; b – oblong elliptical

For such configurations, the Doppler frequency is determined by Equation 5

$$f_D = -\frac{N_n}{\lambda_0}. \quad (5)$$

Figure 6 shows the functional diagram of the experimental FOAES.

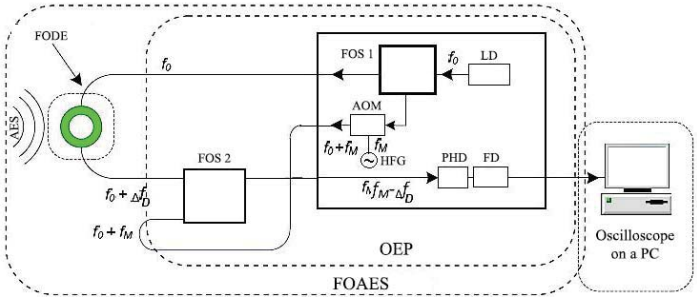

Figure 6. Functional diagram of the experimental FOAES:
FODE – fiber-optic Doppler element; AOM – acousto-optic modulator; FOS – fiber optic splitter; LD – laser diode; HFG – high frequency generator; PHD – photodetector; FD – frequency detector; AES – acoustic emission signal

The Doppler shift frequency f_D (for example, 0.1 Hz ... 1 MHz) is extracted from the optical signal using acousto-optical heterodyning, shifting f_0 by a constant modulation value f_M (for example, 80 MHz), the formation of beats with a frequency $f_D + f_M$, optoelectronic conversion in a photodetector device and converting the frequency deviation f_D into the output signal Uout in the frequency detector.

Adhesive fastening of acoustic emission FOS on the surface of the AC is simple and technologically advanced. With this method of installing FOAES, it is necessary to manufacture a sensor optical cable (SOC) with a Young's modulus of the coating of at least 3 GPa and use an adhesive with an elastic modulus of at least 20 GPa after ultraviolet (UV) curing.

Experimental assessment of the technical characteristics of Doppler FOAES was carried out on test plates: aluminum and composite, as shown in Figures 7 and 8 [4].

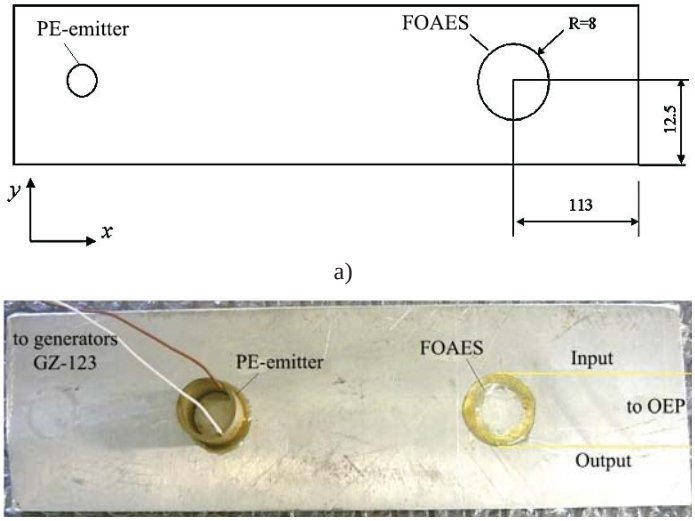

Figure 7. Test aluminum plate for FOAES: a – a diagram for studying the spectra of ultrasonic Lamb waves; b – a real setup for studying the spectra of ultrasonic Lamb waves

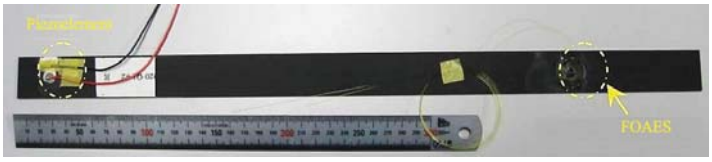

Figure 8. Test composite plate for FOAES

As equipment providing experiments with FOAES according to the scheme of Figure 7, we used: standard generators of the GZ-123 type for exciting piezoelectric emitters from 33 to 170 kHz, a G4-143 high-frequency generator for controlling an acousto-optic signal modulator with a frequency of 80 MHz, broadband amplifiers with an amplification band of up to 500 kHz and frequency detectors for the beat frequency range from 78 to 82 MHz, digital oscilloscopes of the DSO-250 type with built-in software that allows spectral analysis of AE signals using fast Fourier transform. This standard equipment was used to receive AE signals using FOAES Doppler sensors, process them, and display them on a computer screen.

To date, new technical solutions have been developed aimed at simplifying the methods of processing broadband acoustic emission signals, which make it possible to perform FOAES structurally easier and cheaper, with an increased signal-to-noise ratio, due to one conversion of an acoustic-optical signal into an electrical one.

With the help of laser shaping, an optical fiber is micronized, the microscopic image of which is shown in Figure 9.

Figure 9. Microscopic view of optical fiber microcontraction

An acousto-optic frequency shift, a key acousto-optic element, is implemented on the intra-fiber interaction of leaky optical modes: between the mode of the fundamental radiation of a laser diode with a frequency f_0 and a mode modulated with a frequency f_m, using a cone piezoelectric transducer 1 in a microconversion of an optical fiber, as shown in Figure 10.

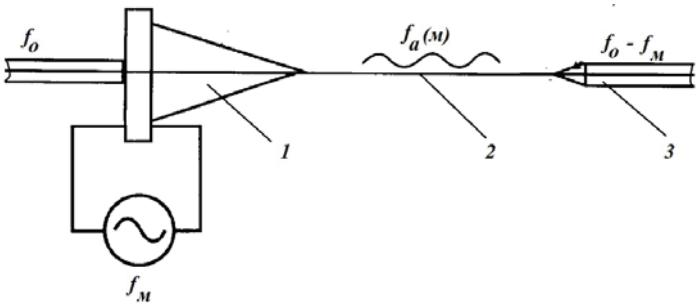

Figure 10. Functional diagram of an acousto-optic generator based on optical fiber micro-narrowing

The interaction of optical modes occurs in the section of the optical fiber 2, with a transverse size of about 10 microns. The frequency of optical radiation in the output fiber $3(f_0 - f_m)$ is shifted by the modulation frequency f_m (for example, by 40 MHz).

The obvious advantages of such an acousto-optic frequency shift (heterodyne): compactness, the absence of adjustable optical collimators for input-output radiation, and an increased signal-to-noise ratio.

Results and their discussion

A study of the AE signals in the time domain, received by the FOAES and the piezoelectric sensor, was carried out. Sample results are shown in Figures 11 and 12.

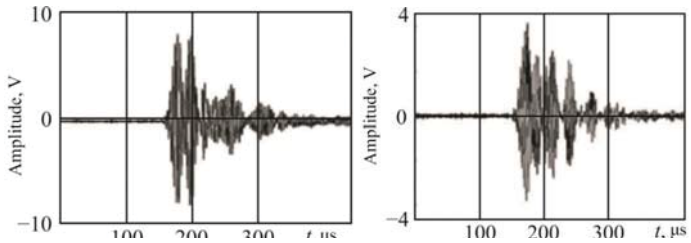

Figure 11. AE signals received by the piezoelectric sensor

Figure 11 shows the signals received by the receiver of acoustic emission signals at various levels of deformation of the internal structure of the material under study, the level of deformation is the smallest in the right figure.

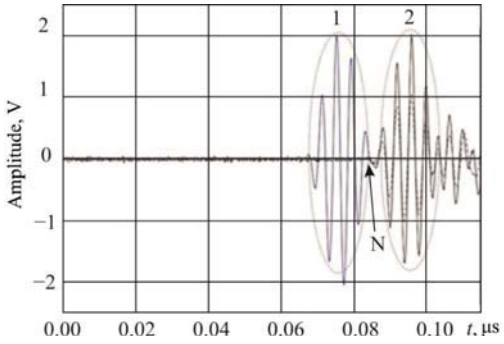

Figure 12. Observation of the FOAES responses to the excited AE signal

As shown in the results of [5], noisy AE signals (Fig. 12) were processed using various methods of digital median filtering, which is reflected in Figure 13.

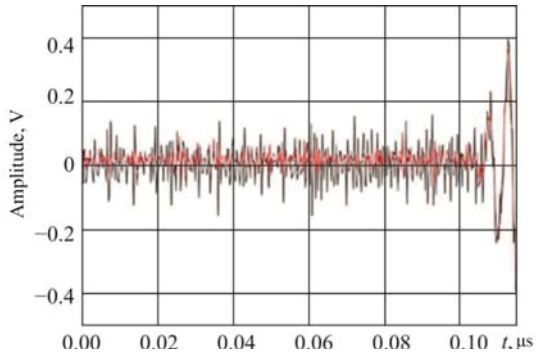

Figure 13. Processing of a noisy AE signal from FOAES

Typical time response and Fourier spectrum of Doppler FOAES acoustic emission from internal delamination of a tubular composite structure is shown in Figure 14.

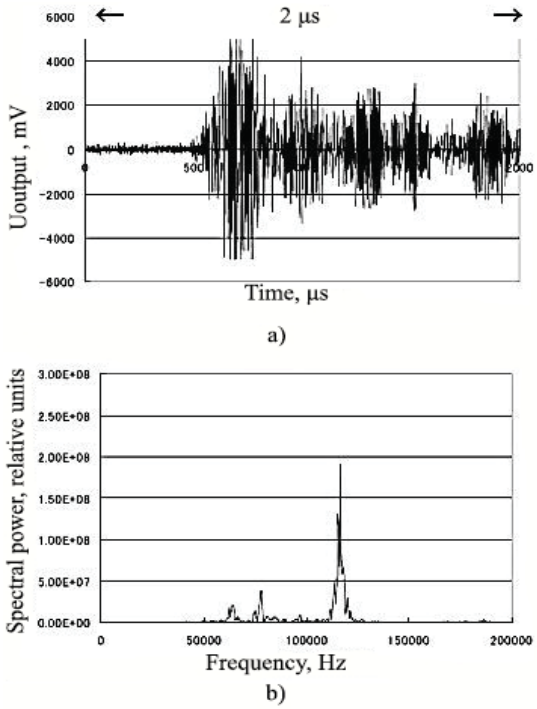

Figure 14. Time (a) and spectral (b) responses of the Doppler FOAES

The results of measuring the amplitude-frequency characteristics of the fiber and piezoelectric AE sensors are shown in Figure 15.

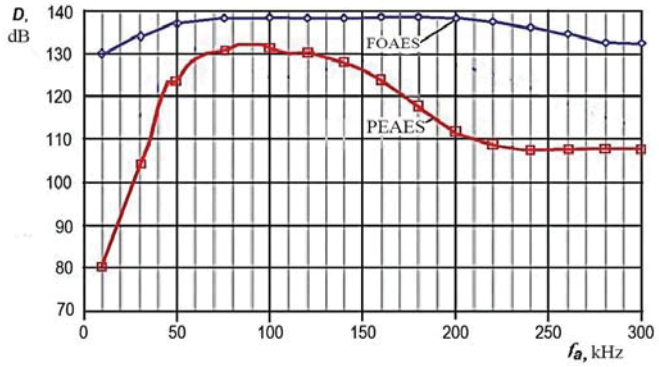

Figure 15. Amplitude-frequency characteristics of the Doppler (FOAE) and piezoelectric (PEAE) sensors

The measurements of the radiation patterns of the annular U-shaped and elliptical FOAES gave the results shown in Figure 16.

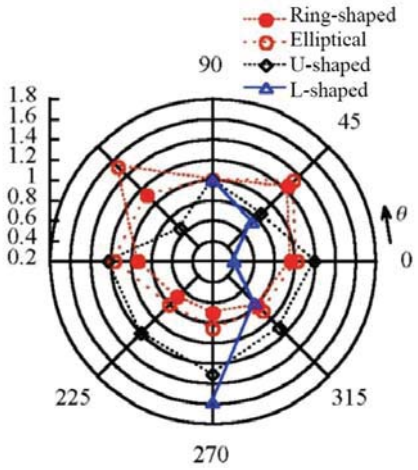

Figure 16. Directional diagrams of FOAES of various shapes

It is obvious that the annular FOAES has a practically non-directional spatial characteristic, and the other two easily manufactured forms have pronounced directional properties. The direction of 90º is taken as a unit in Figure 3.97.

The measurement results showed that:

1) a ber-optic AE sensor based on the intra-light Doppler effect, fixed on the plate, recorded elastic vibrations in the plate wall, excited by piezoceramic transducers at frequencies f from 10 kHz to 300 kHz;

2) a decrease in the excitation level showed that the FOS sensitivity threshold (a distinguishable response to oscillations of the pipe wall $\varepsilon = 10^{-5}$ mln^{-1}) is at the level of 15 μV;

3) the technical solutions incorporated in the investigated FOAES provide a positive dynamics of the transformation of the sensor nodes if it is necessary to increase the sensitivity to ultrasonic vibrations by increasing the length of the annular Doppler element from 10 to 50 m, which will increase the sensitivity by 5 times.

Currently, large-scale studies of the physical characteristics of Bragg gratings are underway, which make it possible to significantly expand their application areas [6]. The spectral characteristics of fiber-optic Bragg gratings are resonant, but the wavelength-to-amplitude conversion function for their estimation in the resonance region either oscillates or has a rather flat or nonlinear character. Therefore, to increase the measurement resolution, a FOBG with spectrum inhomogeneities or a FOBG with a special shape of the spectrum is synthesized to ensure linearization of the measurement characteristics. At present, FOBG with concave, triangular symmetric and asymmetric spectrum shapes are being actively developed in the structure of fiber-optic sensors.

The propagation of light in an optical fiber with a short-period and long-period Bragg cell is shown in Figure 17.

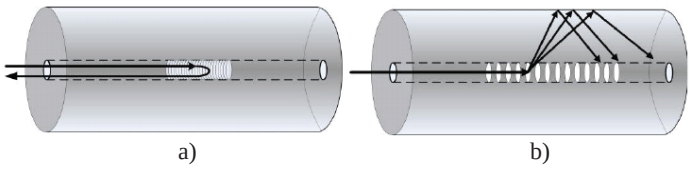

Figure 17. Propagation of light in an optical fiber:
a – with a low-period Bragg cell; b – with a long-period Bragg cell

For inclined Bragg grating (IBG), the light coupling mechanism can also be described using the ray tracing method as shown in Figure 18.

As can be seen from Figure 18, a, when the gratings are inclined at an angle less than 45º, the grating is able to connect the forward propagating mode of the core in the reverse propagating mode of the shell. At 45º, as in the unique case, the core mode will be coupled in the emission mode along the normal to the fiber axis (see Figure 18, b). At an angle tilt of more than 45º, both the ING and the partially inclined Bragg cell (PIBC) are able to connect the forward propagating mode of the nucleus into the progressively propagating mode of the shell, but of a higher order (see Fig. 18, c).

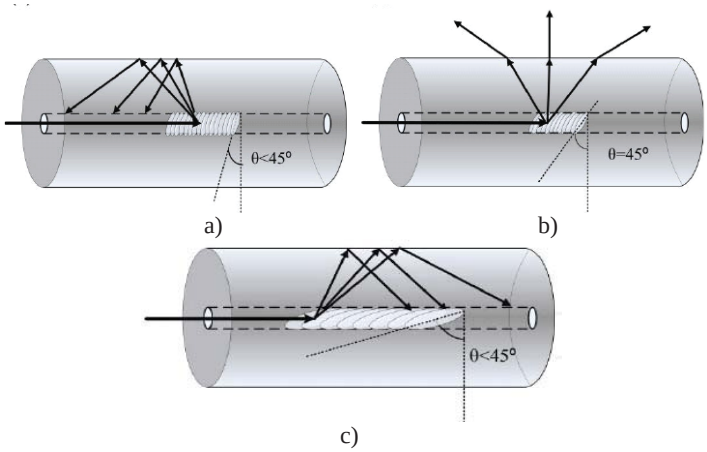

Figure 18. Explanation of the method of ray tracing in optical fiber:
a – the angle of inclination is less than 45º; b – the angle of inclination is 45º;
c – the angle of inclination is more than 45º

The phase matching condition of the IBG can be depicted in the vector plane, which is shown in Figure 19, where θ indicates the angle of inclination of the grating with respect to the fiber axis.

From Figure 3.100, a we can conclude that at this position of the angle, the slope is reduced to zero and the phase matching develops under standard FOBG conditions, from which the forward propagating mode was connected in an identical mode of the backward propagating mode through Bragg diffraction gratings. Figure 19,b shows a special case of 45° – IBG, which are able to connect from indicators perpendicular to the fiber axis or the direction of propagation of the incident beam. At the same time, Figure 19,c shows the mechanism of the incident light beam in the mode of excessively forward propagation, which is called the structure of the grating. Although the phase matching condition provides a very good approximation for interpreting the mode coupling mechanism within the IBG, this does not entail the polarization effect, which is actually one of the key properties of the IBG.

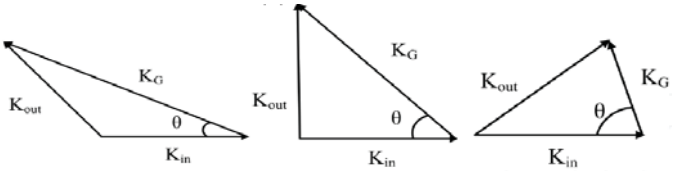

Figure 19. Vector description of phase matching conditions for ING with angles: a – <45°; b – 45°; c – > 45°

Due to the large slope of the induced asymmetry angle to the fiber geometry, the PIBC generates splitting-dependent polarization that shows pairs of vertices corresponding to two orthogonal polarization modes. In this way, the equivalent fast axis and slow axis can be defined similar to the traditional retention of polarization of the fiber structure, as shown in Figure 20.

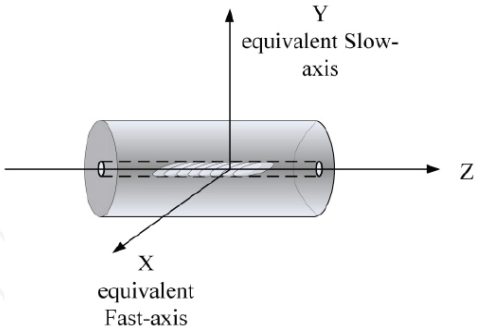

Figure 20. Schematic representation of the PIBC structure with two orthogonal polarization axes

It is this distinctive polarization mode of the splitting mechanism that makes the PIBC ideal as refractive load index sensors [7] and torsion sensors [8] based on the polarization property and using the intrinsic sensitivity of high order modes in the environment.

Partially tilted Bragg cells showed a low thermal sensitivity equal to 3.3 μm/ºC in the 1200 nm range [9]. Thermal sensitivity in the 1550 nm range is of interest for the use of optical sensors. The thermal sensitivity of the PIBC was examined by installing a Peltier grating onboard heat exchanger using a commercial temperature controller, controlling the change in the transmission spectrum with elevated temperature. We studied two pairs of the PIBC peak loss at about 1560 nm and 1610 nm separately.

Figure 21 shows the dependence of the shear wavelength of two paired loss peaks as the grating temperature increases from 20°C to 80°C in 10°C steps.

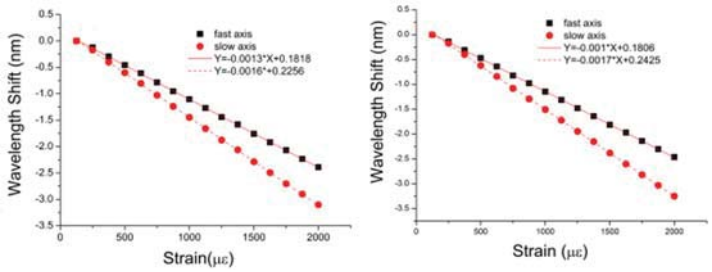

Figure 21. The wavelength of the shift of two paired peaks of losses of PIBC against temperature changes in the ranges around: a – 1560 nm; b – 1610 nm

Compared to conventional IBG [10], PIBC exhibits significantly lower sensitivity to temperature, so PIBC can be an ideal optical sensor without a mandatory temperature compensation circuit.

The properties of the PIBC, due to the change in the parameters during twisting, make it possible in the future to use them as sensors of rotations of nodes.

Since the polarization of the PIBC depends on the contact of the sensor with the polarized light, the polarization of the direction of the light will change if the fiber is twisted. The PIBC diagram of the torsion stress perception is shown in Figure 22.

One side of the PIBC is clamped in a metal block, and the other side of the PIBC is fed to the signal receiver through a fiber rotator. The length between the fiber clamp and the fiber rotator is *L*.

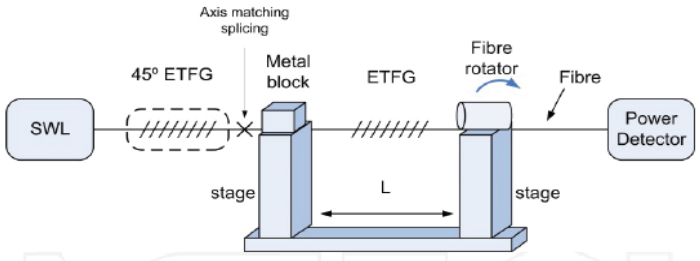

Figure 22. Schematic description of the experimental setup all-fiber lattice based on sensor rotation system: SWL – laser source; Power Detector – power detector; stage – basic; 45º ETFG – fiber optic with 45° grids; Fiber – fiber optic; Fiber rotator – twisting the fiber

To eliminate axial deformation and bending effects of the optical fiber, apply a small amount of force to reduce the measurement error. Before starting to measure the bend, you need to make sure that the zero degree of rotation is normalized in such a state that the axis mode is fully excited by adjusting the PC. Then rotation was applied to the grating in a clockwise direction from 0º to 180º in 10º increments. The resulting evolution of the transmission spectra is shown in Figure 23. It clearly shows that when the PIBC is under bending, the strength of the fast axis modes increases, while the slow axis mode decreases. More importantly, the fast axis mode is reduced completely when the steering angle is 180º. Reverse changes were observed when

rotation was applied counterclockwise from 0° to 180° between fast axis and slow axis modes.

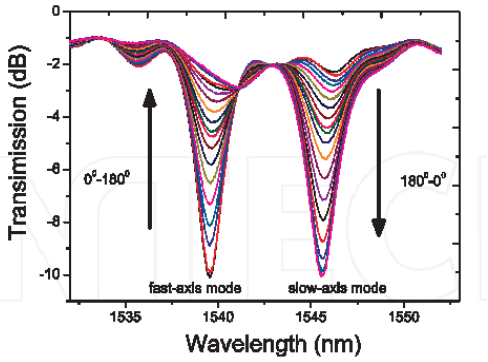

Figure 23. Resultant evolution of transmission spectra upon fiber twisting

The unusual properties of fiber can be applied to measure loads.

Taking a standard single-mode fiber with a cylindrical geometry for the experiment, when a shear force is applied to the y-axis, as shown in Figure 24, for a given compressive force F, the stresses in the x and y directions can be expressed as

$$\sigma_x = \frac{2F}{\pi DL} \text{ and } \sigma_y = \frac{6F}{\pi DL}, \quad (6)$$

where D – the fiber diameter; L – the length of the stress region; F – the force applied to the fiber.

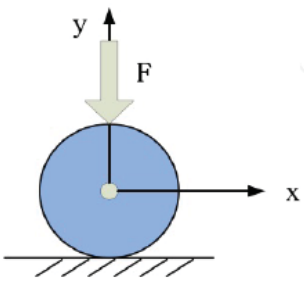

Figure 24. Cross-section of a fiber in a fixed x-y coordinate system with a transverse load applied along the y-axis

It should be noted that δ_x – tensile stress is positive, while δ_y – ompression stress, which is negative, therefore $(\delta_x - \delta_y) > 0$ is always true. The photoelastic induced effect of a change in the refractive index in the region of the fiber core can be specified [11]:

$$\Delta n = n_x - n_y = \left(n_{x0} - n_{y0}\right) + \left(C_1 + C_2\right)\left(\delta_x - \delta_y\right), \quad (7)$$

where n_{x0} and n_{y0} – the effective refractive indices of the fiber without stress; C_1 and C_2 – optical voltage coefficients; the ratio $(C_1 - C_2) > 0$ is always true for silica fiber [12].

If the lateral load is applied in the slow axis in the CNBR, we will have $n_{x0} = n_f$ and $n_{y0} = n_s$, where nf and ns- refractive indices for a predetermined fast and slow axis of the PIBC. Consequently, the first term in equation (3.18) will be negative, which will lead to a decrease in birefringence Δn. In this situation, it is expected that the light coupling of the two orthogonal polarized modes tends to be dependent on the external load. Conversely, if the lateral load is applied in the direction of the fast axis, we will have $n_{x0} = n_s$ and $n_{y0} = n_f$... Thus, we will have a positive value in the first term of equation (7), which will lead to an increase in birefringence Δn. In this case, the PIBC is able to provide decoupling of two orthogonal polarized modes.

In the experiment, a lateral load was applied on the slow axis of the PIBC from 0 to 2600 g with a step of 200 g. The evolution of the spectrum is shown in Figure 25.

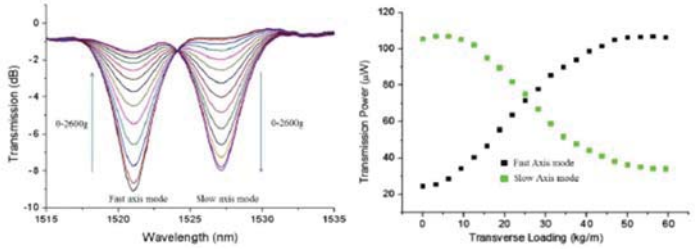

a) b)

Figure 25. Transmission of the evolution of the spectrum of the PIBC (a) with a lateral load from 0 to 2600 g, applied on the slow axis of the PIBC and an auxiliary fiber, and the evolution of the power supply of the PIBC load sensor (b) using the power meter

Figure 25 clearly shows that with an increase in the weight of the load, the intensity of the fast axis mode increases, while in the slow axis mode it decreases. It is noted that when the load is applied to the fast axis of the PIBC, the spectrum does not evolve. This unique property can potentially serve as a vector load cell that is capable of not only measuring load amplitudes, but also identifying the direction of the load.

Conclusion

Based on the above, the following conclusions can be drawn: for the implementation of the tasks in the field of diagnostics of the technical condition of the airframe and the main mechanical assemblies, sensors with minimum weight and dimensions and power consumption should be used. These promising sensors include fiber-optic sensors with distributed Bragg cells, which make it possible to monitor the stress-strain states of the airframe and the main mechanical components. On the basis of such sensors, it is very promising to develop technical means that allow monitoring the dynamics of internal deformations of controlled units and assemblies in real time, based on measuring the spectrum of internal accelerations of loaded units of the airframe and main units, taking into account phase relationships.

The development of the method for diagnosing the stress-strain states of the airframe and the main units of aircraft complexes is a method based on the use of frequency-Doppler fiber-optic sensors having a significantly high signal-to-noise ratio with sufficient broadband with a spherical directional pattern.

The final diagnostics, carried out on the ground after the flight, is advisable to be carried out on the basis of eddy current sensors, which have a very large penetration depth for detecting hidden defects.

Fiber-optic Bragg sensors with an inclined array should be considered as promising areas of research in the field of creating new sensors with new physical properties. These sensors, with the unique polarization mode separation property, have featured

vector detection functions such as loading and twisting sensors. This makes it possible not only to measure the loading and twisting amplitudes, but also to determine the direction of the measured values.

References

1. W. Staszewski, C. Boller, G.R. Tominson (2004). Health monitoring of aerospace structures: smart sensor technologies and signal processing. New York: Wiley, 2004. 266 p.
2. G. Ya. Buimistryuk, V. Nikolaev (2012). New principles and technological possibilities of constructing fiber-optic hydroacoustic sensors and antennas. *Proceedings of the XI All-Russian. conf. «Applied technologies of hydroacoustics and hydrophysics»*. SPb. P. 344-352.
3. H. Guo, G. Xiao, N. Mrad (2011). Fiber optic sensors for structural health monitoring of aircraft platforms. *Sensors*. No 11. P. 3687-3075.
4. X. Chen, K. Zhou, L. Zhang et al. (2006). In-fiber twist sensor based on a fiber Bragg grating with 81 Tilted structure. *IEEE Photonics Technology Letters*. Vol. 18, No. 24. P. 2596-2598.
5. K.M. Zhou, L. Zhang, X.F. Chen et al. (2006). Low thermal sensitivity grating devices based on Ex-45 degrees tilting structure capable of forward-propagating cladding modes coupling. *J. Lightwave Technol*. Vol. 24, no. 12. P. 5087-5094.
6. S.W. James, R.P. Tatam (2003). Optical fiber long-period grating sensors: characteristics and application. *Measurement Science and Technology*. Vol. 14. P. 49-R61.
7. N. Imoto (1980). Birefringence in Single-Mode Optical Fiber Due to Elliptical Core Deformation and Stress Anisotropy. *IEEE J. Quantum Elect*. Vol. 16, no. 11. P. 1267.
8. I. E. Mukhin (2014). The main directions of development of systems for diagnostics and prognostics of the technical condition of aircraft. *Materials of the VI scientific-practical conference «Flight data accumulators, predictive and diagnostic systems, on-board measurements»*. Kursk: JSC «Aviaavtomatika» named after V. V. Tarasov», pp. 35-37.
9. I.E. Mukhin (2014). The main directions of development of systems for diagnostics and prognostics of the technical state of aircraft. *Innovations*. No. 9. P. 110-113.
10. I.E. Mukhin, S.L. Seleznev, D.S. Koptev (2017). Directions and practical results of creating methods and means of diagnostics and prognostics of the state of the aviation complex «man-machine». *Izvestiya Yugo – Western State University*. Vol. 7. No. 3 (24). P. 46-58.
11. S. Arajs, C.A. Moyer, K.W. Brown (1978). Determination of the ferromagnetic Curie temperature for $Fe_{40}Ni_{40}P_{14}B_6$ (Metglas 2826). *Physica Scripta*. Vol. 17. P. 543.
12. P.S. Popovic (2003). Hall effect devices. Second ed. CRC Press. P.42.

ПРАКТИЧЕСКИЕ РЕЗУЛЬТАТЫ И ПЕРСПЕКТИВЫ ИСПОЛЬЗОВАНИЯ ВОЛОКОННО-ОПТИЧЕСКИХ ДАТЧИКОВ АКУСТИЧЕСКОЙ ЭМИССИИ ДЛЯ ДИАГНОСТИКИ ТЕХНИЧЕСКОГО СОСТОЯНИЯ АГРЕГАТОВ ЛЕТАТЕЛЬНЫХ АППАРАТОВ

Коптев Дмитрий Сергеевич, *Юго-Западный государственный университет, г. Курск, Россия,* ***d.s.koptev@mail.ru***
Мухин Иван Ефимович, *Юго-Западный государственный университет, г. Курск, Россия,* ***makskatol21@yandex.ru***

Аннотация

Периферийные датчики для снятия параметров летательных аппаратов являются неотъемлемой частью любой системы диагностики и прогностики технического состояния. Их принцип работы применительно к эксплуатации на авиационных комплексах заключается в преобразовании механических, электромагнитных или световых величин в электрические для их последующей обработки. Процесс излучения распространяющихся в материале возмущений, вызванных динамической локальной перестройкой структуры материалов под действием внутренних напряжений, приводящих к изменению кристаллической решетки или движению микро- и/или макродефектов носит название акустической эмиссии. Так, анализ отличий в форме акустических волн позволяет осуществлять классификацию вида деформаций: трещина или пластическая деформация, что позволяет более точно определять текущее состояние планера или диагностируемых узлов. Принцип работы таких датчиков основан на эффекте преобразования линейных размеров ячейки Брэгга, выполненной на оптоволокне, в изменение отраженной длины волны. Необходимым условием получения корректных результатов измерений напряженных состояний является необходимость температурной компенсации ячеек Брэгга, что достигается введением дополнительных ячеек, механически развязанных от диагностируемого материала и реагирующих только на температурную составляющую. Достоинством этого метода является отсутствие необходимости дополнительной настройки ячеек и их юстировки, а также независимость измерений от воздействия электромагнитных излучений; датчики же обладают малой массой, устойчивы к вибрациям, нечувствительны к электромагнитным полям. В статье представлены практические результаты использования волоконно-оптических датчиков акустической эмиссии для диагностики технического состояния ответственных узлов и агрегатов летательных аппаратов, а также изложены перспективы их наиболее глубокой интеграции в единую информационно-аналитическую систему диагностики и прогностики технического состояния авиационных комплексов. Представлены проработанные технические решения, направленные на упрощение способов обработки широкополосных акустоэмиссионных сигналов, которые позволяют выполнять датчики акустической эмиссии на основе оптоволокна конструктивно проще и дешевле, с повышенным отношением сигнал/шум, за счёт одного преобразования акустико-оптического сигнала в электрический.

Ключевые слова: *акустическая эмиссия, волоконно-оптический датчик акустической эмиссии (ВОДАЭ), эффект Доплера, волоконно-оптические решётки Брэгга (ВОБР), наклонная брэгговская решетка (НБР), частично наклоненная ячейка Брэгга (ЧНБР).*

Литература

1. *Staszewski W., Boller C., Tominson G. R.* Health monitoring of aerospace structures: smart sensor technologies and signal processing. New York: Wiley, 2004. 266 p.
2. *Буймистрюк Г.Я., Николаев В.* Новые принципы и технологические возможности построения волоконно-оптических гидроакустических датчиков и антенн // Труды XI Всерос. конф. "Прикладные технологии гидроакустики и гидрофизики". СПб., 2012. С. 344-352.
3. *Guo H., Xiao G., Mrad N.* Fiber optic sensors for structural health monitoring of aircraft platforms // Sensors. 2011. No 11. P. 3687-3075.
4. *Chen X., Zhou K., Zhang L.* et al. In-fiber twist sensor based on a fiber Bragg grating with 81 Tilted structure // IEEE Photonics Technology Letters. 2006. Vol. 18, no. 24. P. 2596-2598.
5. *Zhou K.M., Zhang L., Chen X.F.* et al. Low thermal sensitivity grating devices based on Ex-45 degrees tilting structure capable of forward-propagating cladding modes coupling // J Lightwave Technol. 2006. Vol. 24, no. 12. P. 5087-5094.
6. *James S.W., Tatam R.P.* Optical fibre long-period grating sensors: characteristics and application // Measurement Science and Technology. 2003. Vol. 14. P. R49-R61.
7. *Imoto N.* Birefringence in Single-Mode Optical Fiber Due to Elliptical Core Deformation and Stress Anisotropy // IEEE J. Quantum Elect. 1980. Vol. 16, no. 11. P. 1267.
8. *Мухин И.Е.* Основные направления развития систем диагностики и прогностики технического состояния летательных аппаратов // Материалы VI научно-практической конференции "Накопители полетных данных, системы прогностики и диагностики, средства бортовых измерений". Курск: ОАО "Авиаавтоматика" имени В. В. Тарасова", 2014. С. 35-37.
9. *Мухин И.Е.* Основные направления развития систем диагностики и прогностики технического состояния летательных аппаратов // Инновации. №9. 2014. С. 110-113.
10. *Мухин И.Е., Селезнев С.Л., Коптев Д.С.* Направления и практические результаты создания методов и средств диагностики и прогностики состояния авиационного комплекса "человек – машина" // Известия Юго-Западного государственного университета. 2017. Т. 7, №3(24). С. 46-58.
11. *Arajs S., Moyer C.A., Brown K.W.* Determination of the ferromagnetic Curie temperature for Fe40Ni40P14B6 (Metglas 2826) // Physica Scripta. 1978. Vol. 17, is. 5. P. 543.
12. R.S. Popovic. Hall effect devices. Second ed. CRC Press, 2003. 420 p.

Информация об авторах:

Коптев Дмитрий Сергеевич, *старший преподаватель кафедры космического приборостроения и систем связи, Юго-Западный государственный университет, г. Курск, Россия*

Мухин Иван Ефимович, *д.т.н., с.н.с., профессор кафедры космического приборостроения и систем связи, Юго-Западный государственный университет, г. Курск, Россия*